Scientific Research Publishing

Journal of Geoscience and Environment Protection, 2024, 12, 40-59
https://www.scirp.org/journal/gep
ISSN Online: 2327-4344
ISSN Print: 2327-4336

Simultaneous Waveform Inverse Modelling for Litho-Fluid Prediction in an Old Marginal, "Agbbo" Field, Onshore Niger Delta, Nigeria

Charles Chibueze Ugbor[1*], Peter Ogobi Odong[1], Chukwuemeka Austine Okonkwo[2]

[1]Department of Geology, University of Nigeria, Nsukka, Nigeria
[2]Department of Geology and Mining, Enugu State University of Science and Technology, Enugu, Nigeria
Email: *charles.ugbor@unn.edu.ng

How to cite this paper: Ugbor, C. C., Odong, P. O., & Okonkwo, C. A. (2024). Simultaneous Waveform Inverse Modelling for Litho-Fluid Prediction in an Old Marginal, "Agbbo" Field, Onshore Niger Delta, Nigeria. *Journal of Geoscience and Environment Protection, 12,* 40-59.
https://doi.org/10.4236/gep.2024.125003

Received: December 20, 2023
Accepted: April 17, 2024
Published: May 20, 2024

Abstract

Simultaneous waveform inversion was used to predict lithofacies and fluid type across the field. Very often, characterizing reservoirs in terms of lithology and fluid type using conventional methods is replete with uncertainties, especially in marginal fields. An approach is employed in this study that integrated rock physics and waveform inverse modelling for lithology and fluid-type characterization to appropriately identify potential hydrocarbon saturated zones and their corresponding lithology. Seismic and well-log data were analyzed using Hampson Russel software. The method adopted includes lithofacies and fluid content analysis using rock physics parameters and seismic simultaneous inverse modelling. Rock physics analysis identified 2 broad reservoirs namely: HDZ1 and HDZ2 reservoirs. Results from the inverse modelling showed that low values of acoustic impedance from 19,743 to 20,487 (ft/s)(g/cc) reflect hydrocarbon-bearing reservoirs while medium to high values shows brine and shale respectively, with brine zone ranging from 20,487 to 22,531 (ft/s)(g/cc) and shale above 22,531 (ft/s)(g/cc). Two lithofacies were identified from inversion analysis of Vp/Vs and Mu-Rho, namely: sand and shale with VpVs < 1.95 and >1.95 values respectively. Mu-Rho > 12.29 (GPa)(g/cc) and <12.29 (GPa) (g/cc) represent sand and shale respectively. From 3D volume, it was observed that a high accumulation of hydrocarbon was observed to be saturated at the north to the eastern part of the field forming a meandering channel. Sands were mainly distributed around the northeastern to the southwestern part of the field, that tends to be away from Well 029. This was also validated by the volume of rigidity modulus (Mu-Rho) showing high values indicating sands fall within the northeastern part of the field.

Keywords

Simultaneous Waveform Inversion, Lithofacies, Fluid Type, Rock Physics, Hydrocarbon, Acoustic Impedance, Mu-Rho, Reservoir

1. Introduction

It is critical to predict lithology and fluid type using existing data in an old field. In the Niger Delta basin, the quest for more hydrocarbon reservoirs has been tilted to the shelf and deep marine environment (offshore). This is because of the tremendous and continuous reduction of hydrocarbon production in the onshore basins. Because of the high cost of operation in a deep-water environment, this necessitated the use of new technologies and ideas to return to the old and abandoned marginal onshore oil abandoned fields to predict lithofacies and the fluid type to properly track hydrocarbon-bearing zones. Accurate prediction of lithofacies and fluid type has posed a great challenge to subsurface geologists and geophysicists working in the field discovered in the late 1950s with oil production from 1961 (old oil fields) onshore Niger delta basin (Okeugo et al., 2018). Different methods had been used for reservoir evaluation in the Niger Delta. A typical example is the work of Eze et al. (2013) and Ugbor (2023) who evaluated the reservoir from seismic and petrophysical data. Similarly, in their study, llo et al. (2022) used both well log and seismic data to characterize the hydrocarbon reservoir at "Famito" field, Niger Delta, Nigeria. The method gave insight into the reservoir properties with limited information on fluid prediction in the reservoir. Similarly, Ugbor and Onyeabor (2023) evaluated the success of spectral decomposition technique in assessment of a hydrocarbon reservoir in the coastal swamp of the Niger Delta Basin. Also, Ugbor et al. (2023) established the prospectivity and risking of a hydrocarbon reservoir in the Nigeria Delta using both seismic and petrophysical data. These methods could identify a hydrocarbon prospect and quantify the hydrocarbon in place based on available data, but additional information from the current study, integrating the inversion of the seismic waveform could further bridge the uncertainty and enhance the understanding of the hydrocarbon reservoir.

Advancement in seismic technology has led to numerous methods for predicting lithology and fluid type in a reservoir and across the entire field. These methods include simultaneous inversion, stochastic inversion, model base post-stack inversion, elastic impedance inversion, Poisson's impedance inversion, lambda-mu-rho inversion, rock physics template modelling etc., for lithology and fluid prediction (Ekwe et al., 2012; Tian et al., 2010; Farfour et al., 2015; Okeugo et al., 2018; Akpan et al., 2021). The use of pre-stack simultaneous inversion has helped in lithology and fluid type prediction, reducing uncertainties caused by using existing ideas with minimal error. This requires great skills and acquaintance with the data set and understanding the behaviours of the seismic wave-

form on boundaries of impedance contrast.

Many studies have been carried out to transform seismic reflection data into a quantitative rock property (seismic inversion) to describe the reservoir in terms of lithology and fluid type. These studies include a model-based inversion (Horsfall et al., 2014; Othman et al., 2015), Poisson impedance inversion (Okeugo et al., 2018; Akpan et al., 2021), deterministic and geostatistical inversion (Omudu et al., 2007; Nwogbo et al., 2009) for constructing earth models. But one fundamental advantage of using simultaneous waveform inversion is the ability of the inversion process to remove the effect of the wavelet from the seismic data (removal of side lobe and tuning effect introduce by wavelet) and produce a high-resolution image of the surface (Margrave et al., 1998; Veeken & Da Silver, 2004; Moosavi & Mokhan, 2016). Another advantage of utilizing pre-stack seismic waveform inversion in the construction of reliable earth model and lithofacies characterization is the ability of the technique to produce additional information such as shear velocity from the seismic data (Okeugo et al., 2018). However, this additional shear wave velocity information helps in giving better discrimination of reservoir and non-reservoir rocks which is not achieved through the model-based post-stack inversion method (Greenberg & Castagna, 1992; Akpan et al., 2021).

Simultaneous waveform inversion requires accurate estimation of statistical wavelet from both seismic and well data. Accurate wavelet estimation requires a perfect tie of impedance log to the seismic. Error in well tie can result in phase or frequency artifact in the wavelet estimation. Once the wavelet is identified, seismic inversion computes a synthetic log for every seismic trace. To ensure quality, the inverted results are convolved with the wavelet to produce a synthetic seismic trace which is compared to the original seismic. During inversion analysis, all models, partial stack, and wavelet are inputted to a single inversion algorithm enabling inversion to effectively compensate for offset dependent phase, bandwidth, tuning and NMO stretching effect.

Ma (2002) approximation which is an improved version of the Aki Richard approximation was used for the inversion algorithm to find the band limit elastic reflectivities. These were further merged with their low-frequency counterpart model and integrate into elastic properties. The result is then improved in a final inversion of P-impedance, S-impedance, and density subjected to various hard and soft constrain. The algorithm used for this research is based on three assumptions according to Hampson, Russell, & Bankhead, (2005). The first is that linearized approximation for reflectivity holds. The second is that PP and PS reflectivity as a function of angle can be given to the Aki-Richard equation (Aki & Richards, 1980). The third is that there is a linear relationship between the logarithm of P-impedance and both S-impedance and density. From the three assumptions, a final estimate of P-impedance, S-impedance, and density can be found by modifying an initial P-impedance model.

The ability of this method to predict fluids and lithology within the reservoir has produced tremendous and remarkable achievements in the oil and gas industry. Therefore, this research paper is aimed at using simultaneous waveform

inversion for litho-fluid prediction from an old marginal field. The success of this method could be replicated in resolving similar basins elsewhere to enhance more appropriate citing of wells to enhance production.

2. Geology of the Study Area

The study area (Agbbo field) falls within the central swamp depobelt of the Niger Delta basin as shown in **Figure 1**. The Niger Delta basin is situated at the top of the Gulf of Guinea on the west coast of Africa. It is among the most prolific deltaic hydrocarbon provinces in the world. The reservoirs of the field have been dated to Middle Miocene and identified to be deposited in a parasequence of shallow marine and deltaic plain deposits (Reijers, 2011). The delta has one petroleum system called the Akata-Agbada petroleum system of the Tertiary Niger Delta (Chukwuemeka et al., 2018).

It is made up of three lithostratigraphic units, ranging from the oldest Akata Formation, Agbada Formation and the youngest Benin Formation which are all diachronous (**Figure 2(a)**). The Akata Formation is the oldest lithostratigraphic

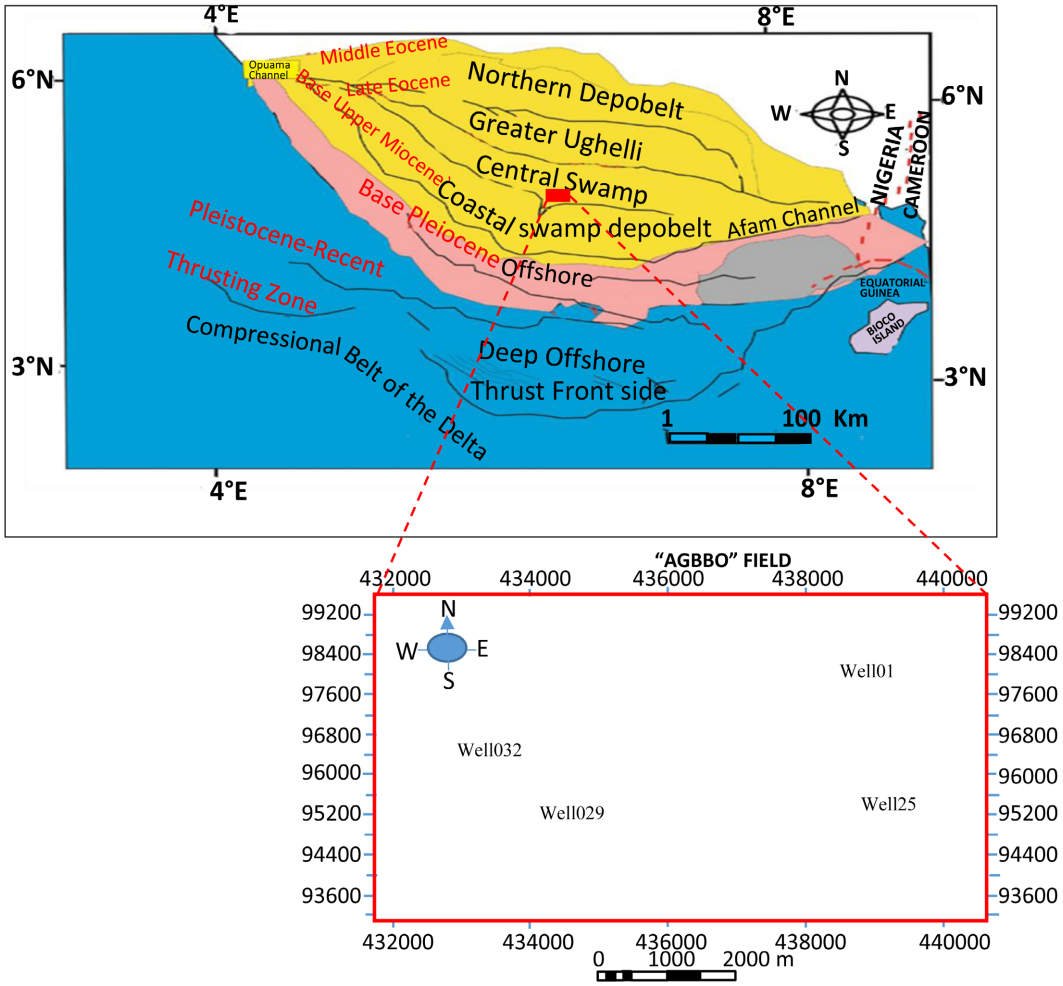

Figure 1. (a) Map of Niger Delta basin showing the location of the study area and depobelts and the study area (modified after Doust and Omatsola, 1989); (b) base map of the study area showing the studied wells.

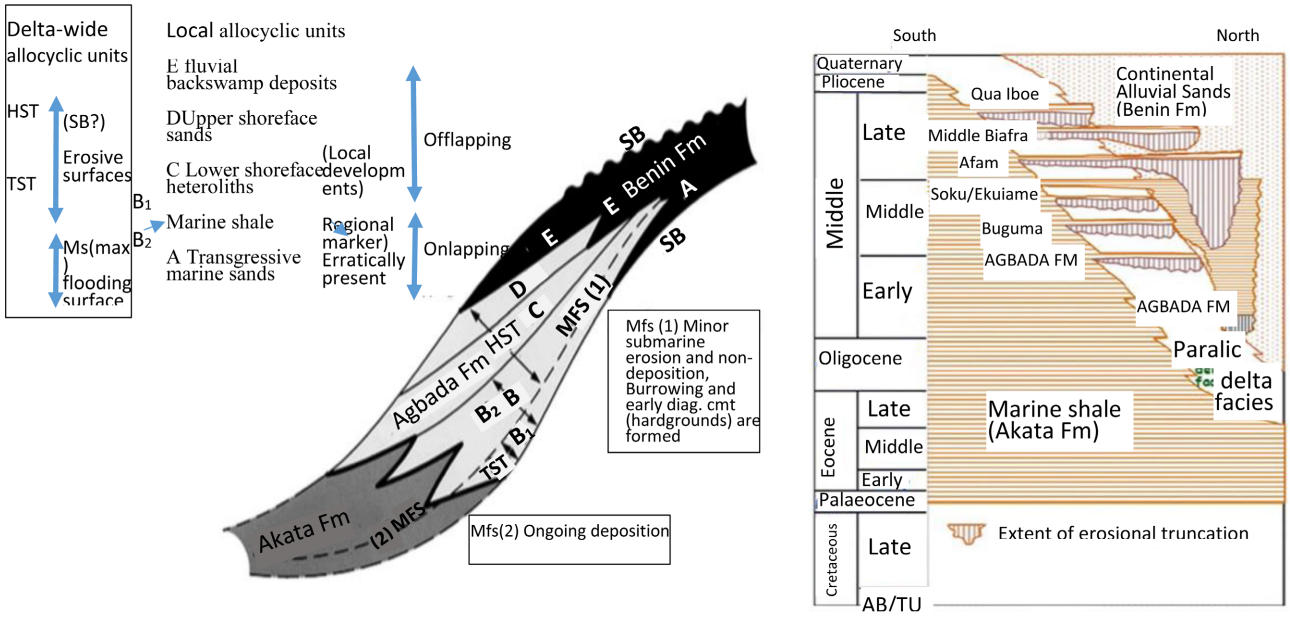

Figure 2. (a) Schematic diagram showing the three allocyclic units of the three formations (adopted from Reijers, 2011). (b) Stratigraphy of the Niger Delta showing the lithologic units of the three formations (adopted from Lawrence et al., 2002).

unit in the Niger Delta. It is aged Paleocene to Recent occurring as a marine sedimentary succession that is laid in front of the advancing delta; it is estimated to be 21,000 feet thick in the central part of the clastic wedge and consists of a thick shale sequence (potential source rock), turbidites sand (potential reservoir in deep waters) and little amount of clay and silt (Doust & Omatsola, 1989). The shales also form diapiric structures including shale swells and ridges which often intrude into the overlying Agbada Formation (**Figure 2(b)**). The agbada formation (paralic clastic) is the second of the three strongly diachronous Niger Delta multifaceted Formations (Short & Stauble, 1967; Frankl & Cordry, 1967). It is characterized by paralic interbedded sandstone and shale with a thickness of over 3000 m (Reijers, 1996). In the Lower Agbada Formation, sand and shale were deposited in equal proportion, while the upper portion is mostly sand with minor shale interbedded. The continental Benin Formation comprises the top part of the Niger Delta clastic wedge, from the Benin-Onitsha area in the north to beyond the coastline (Short & Stauble, 1967). The top of the formation is a recent, sub aerially exposed delta top surface and its base extends to a depth of 4600 feet. The base is defined by the youngest marine shale, while, shallow parts of the formation are composed entirely of non-marine sands deposited in alluvial or upper coastal plain environments during a southward progradation of the delta (Doust & Omatsola, 1989). The schematic diagram is shown in **Figure 2(b)**.

3. Materials and Method of Study

The available dataset used for this study includes a 3-D Prestack Time Migration (PreSTM) seismic volume and suites of wireline log comprising gamma-ray, neutron density, resistivity, and compressional velocity from three wells. The

PreSTM seismic volume and wells were quality-checked (QC) and prepared for the seismic simultaneous inversion process, before loading them into the Hampson Russell 10.1 software for the inversion analysis. A schematic diagram showing the workflow for the study is given in Figure 3.

3.1. Theoretical Background

3.1.1. Pre-Stack Seismic Inversion Waveform Inversion

Pre-stack seismic waveform inversion is an inverse model deconvolution technique used for reservoir property assessment due to its high resolution and ability to identify thin beds and solve an averaging problem. In this paper, the inversion technique is used for obtaining a reliable estimation of earth properties such as acoustic impedance (Zp), Velocity ratio (VpVs), rigidity modulus (Mu-Ro) and Poisson's ratio (PR).

Aki and Richard (1980) gave the first order reflectivity coefficient equation as:

$$R(\theta) \approx \frac{1}{2}\left(\frac{\Delta Vp}{Vp} - \frac{\Delta \rho}{\rho}\right) - 2\left(\frac{Vs}{Vp}\right)^2 \left(2\frac{\Delta Vs}{Vs} + \frac{\Delta \rho}{\rho}\right) \times \sin^2\theta + \frac{1}{2}\frac{\Delta Vp}{Vp}\tan^2\theta \quad (1)$$

Fatti et al., 1994 simplified the equation as

$$R(\theta) \approx \left(1 + \tan^2\theta\right)\frac{\Delta Zp}{2Zp} - 8\left(\frac{Vs}{Vp}\right)^2 \sin^2\theta \frac{\Delta Zs}{Zs} \quad (2)$$

In 2002, Ma made the reflectivity coefficient be a function of only three parameters; Zp, Zs and θ, by replacing Vs/Vp with Zs/Zp in Fatti et al., 1994

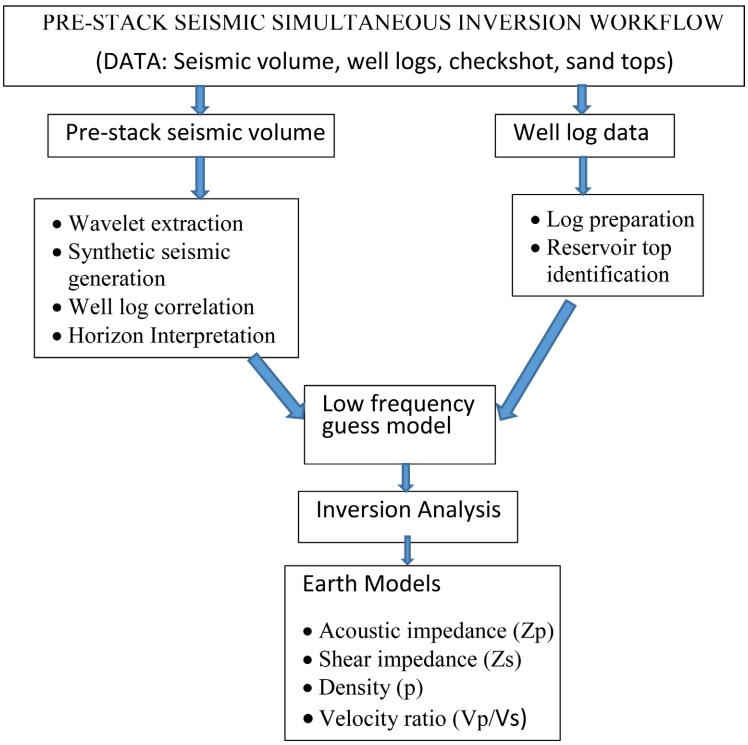

Figure 3. Schematic workflow of simultaneous waveform inverse modelling for Zp, Zs, VpVs and ρ extraction by combined use of seismic and well log data.

$$R(\theta) \approx (1+\tan 2\theta)\frac{\Delta Zp}{2Zp} - 8\left(\frac{Zs}{Zp}\right)^2 \sin^2\theta \frac{\Delta Zs}{Zs} \quad (3)$$

The equation, therefore, forms the foundation of pre-stack seismic simultaneous waveform inversion to estimate acoustic impedance and shear impedance (Zp and Zs) for pre-stack seismic gather.

The procedure is therefore, first to generate the elastic parameters such as acoustic impedance, velocity ratio, mu-rho and Poisson's ratio from the 3D seismic data inversion. This would also normally involve a preconditioning and preparation of a suite of well data such as gamma-ray, resistivity, acoustic impedance, Poisson's ratio, velocity ratio and porosity from well data.

The next stage will be to perform well-to-seismic tie to bring the 2 data sets (seismic and well data) into one unit and to ensure correspondence of the two data sets reflecting that the subsurface reflectors and lithological boundaries tally.

A statistical generated seismic wavelet from the seismic data is used to produce the synthetic seismogram, and from the inversion analysis, an inverted rack each of the following, Zp, Zs, density and VpVs ratio are generated. These are further compared with the original data to ensure no mismatch on the reflectors.

4. Results

4.1. Inversion of Rock Physical Parameters and Well-to-Seismic Tie

The 3D pre-stack seismic data was inverted simultaneously to obtain acoustic impedance, velocity ratio, mu-rho and Poisson's ratio. The inversion started with log preparation, conditioning and reservoir tops identification using the interplay of gamma-ray, resistivity, acoustic impedance, Poisson's ratio, velocity ratio and porosity from well data. The process was carried out for 3 wells, but in this paper, the details of Well 029 are displayed. This is shown in **Figure 4**. Horizon interpretation was carried out to aid the seismic inversion process. Two horizons HDZ1 and HDZ2 were picked at sand packages matching the identified reservoirs from the well data (**Figure 5**). Successful waveform inversion for lithofacies and fluid prediction requires a good estimation of seismic wavelet and a good seismic to well tie with a correlative coefficient of above 70%.

Seismic to well tie was carried out to properly match the well data with the seismic data. The wavelet used for the inversion was estimated statistically from the seismic data. Extracted wavelet was observed to be symmetrical with a maximum at time zero (**Figure 6**).

A synthetic seismogram was also generated in the wells to aid in the inversion. It was observed that the synthetic generated from the well data (blue traces) was not properly matched with the original seismic data (red traces), however, a time sift and stretching of the synthetic to fit the original seismic was required. After this operation was done a good to excellent correlation coefficient of 94.1% was obtained (**Figure 7**). From the inversion analysis, an inverted trace of Zp (track 1) Zs (track 2), Density (track 3) and VpVs ratio (track 4) was obtained. The in-

verted results (in red) overlay the original logs from the well (in blue) and the initial model (black). Analysis of the inverted parameters shows some slide mismatch in the initial, original and inverted model of Zp, Zs, and density, especially at some intervals. Although this did not affect the inverted result (Figure 8). The

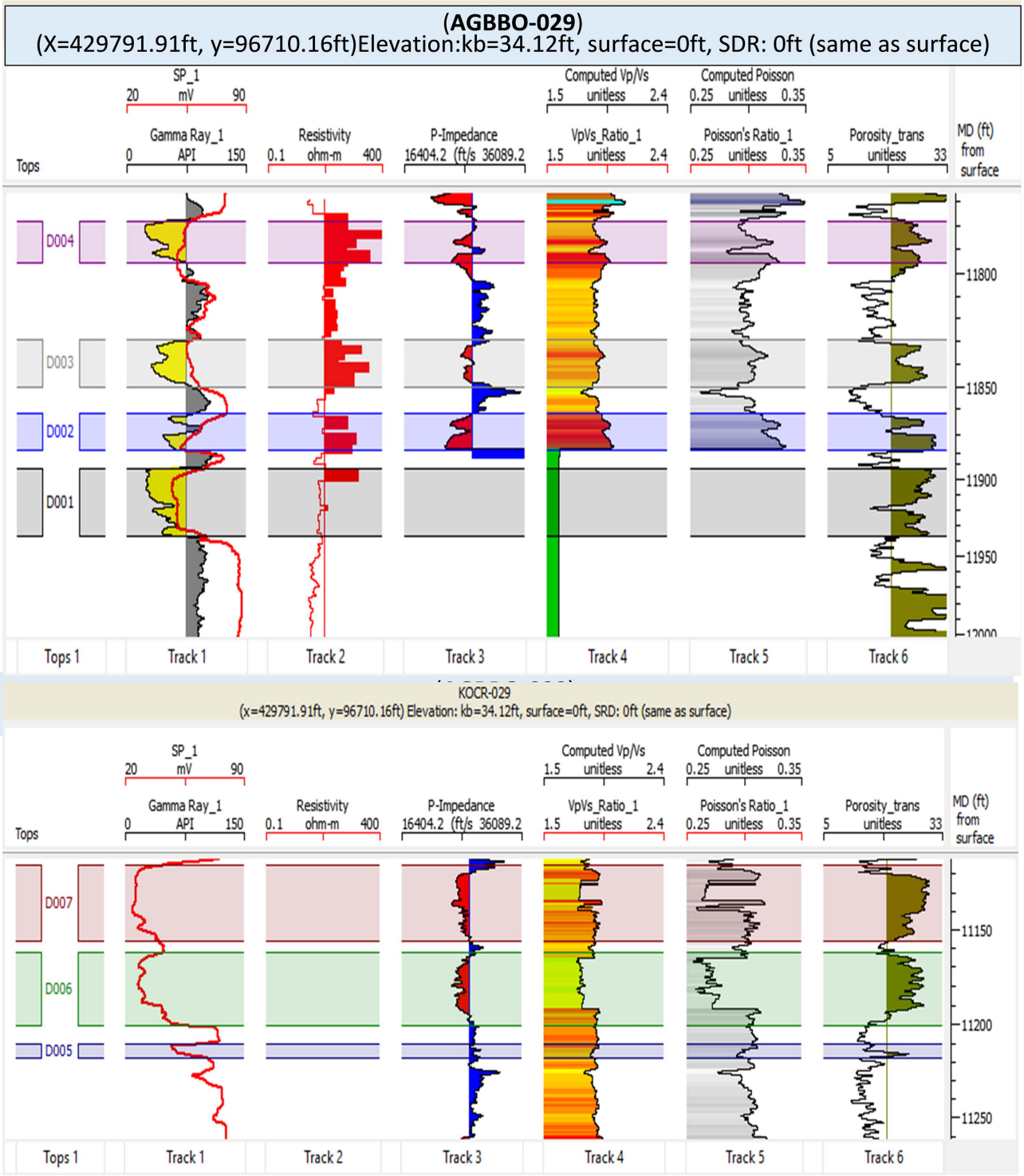

Figure 4. Cross-section of evaluated rock physics parameters of Well 029 showing GR, Resistivity, P-impedance, Vp/Vs ratio, Poisson's ratio and Mu-Rho and the corresponding sub-reservoirs of (a) HDZ2 reservoir and (b) HDZ1 reservoir.

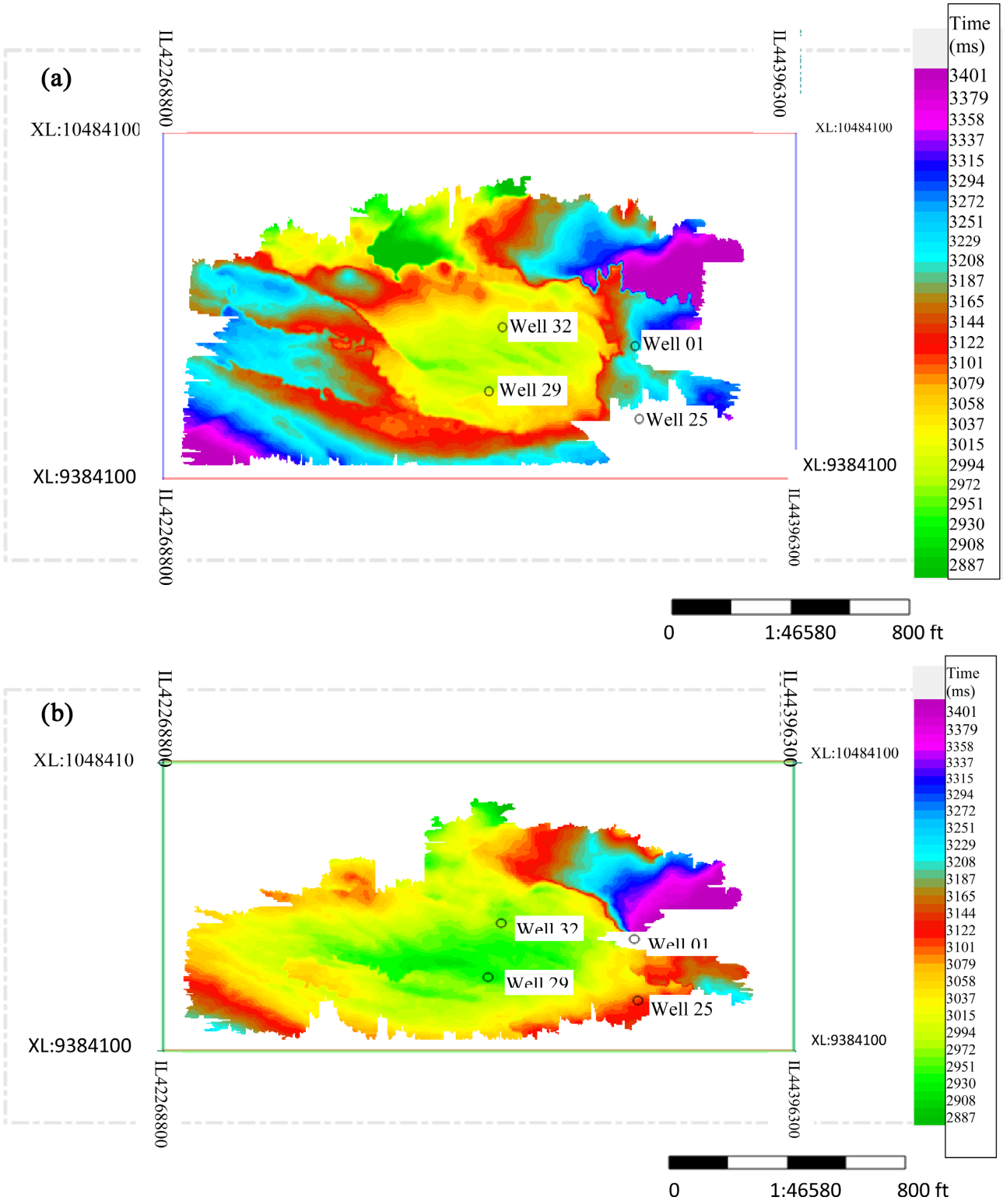

Figure 5. (a) DZ2 horizon time slice b. HDZ1 horizon time slice which cut across HDZ2 and (b) HDZ1 reservoirs respectively used for the inverse modelling process.

error estimated between the density, synthetic and seismic trace remains approximately zero. However, the error gather which is the difference between the

two previous results shows an approximately zero error (0.109).

As expected, the error is small, indicating that the inversion is mathematically correct, i.e. the inversion creates a synthetic trace which matches the real seismic trace. The practical fact behind the observed zero error is that the inversion algorithm has created an impedance trace that is consistent with the extracted wavelet and input seismic trace (Okeugo et al., 2018).

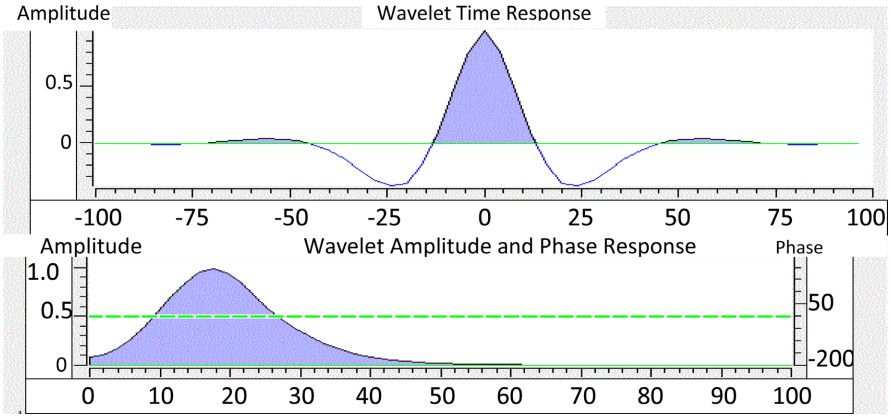

Figure 6. Statistical wavelet extracted from seismic used for seismic inversion showing high amplitude at zero time.

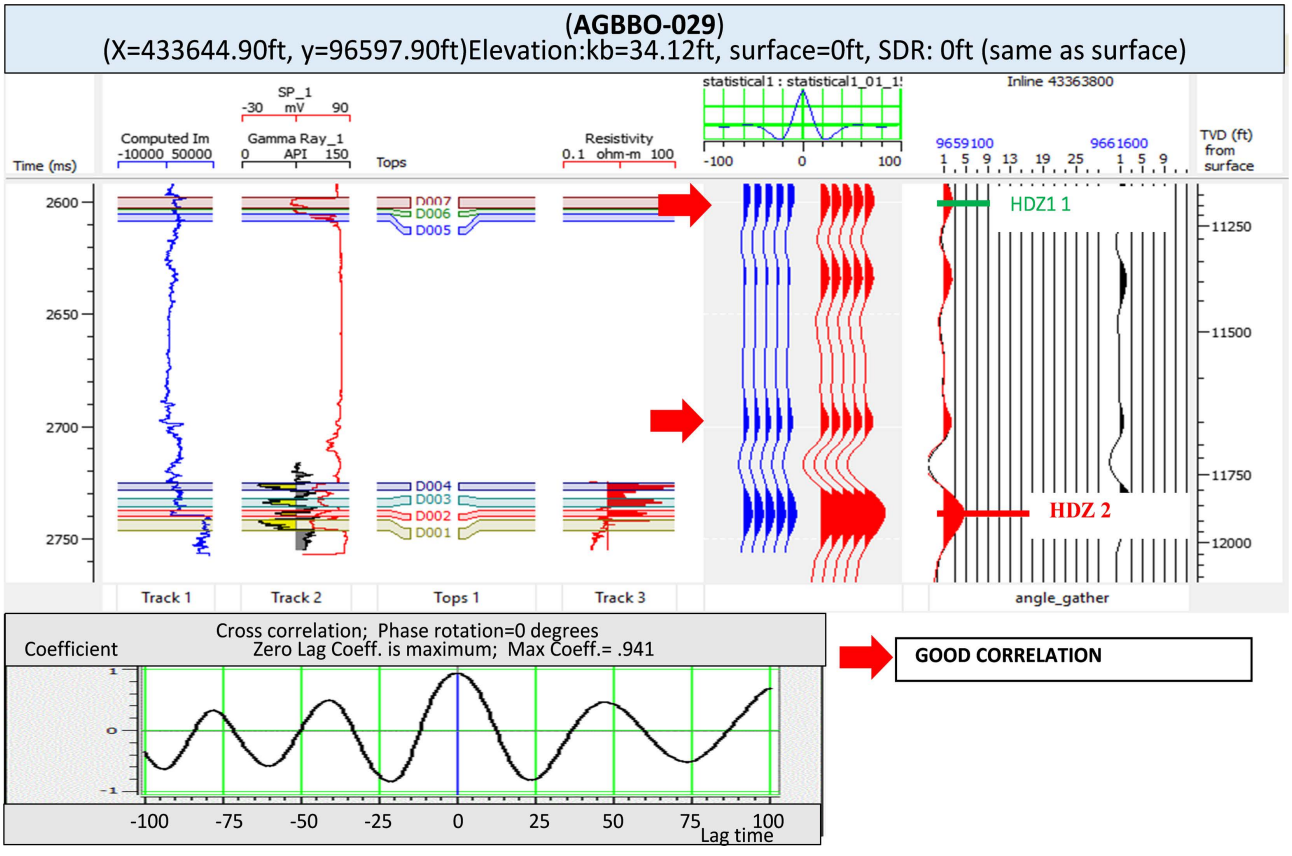

Figure 7. Seismic to well tie of Well 029 showing computed impedance, GR/SP log, well tops, resistivity, synthetic and original seismic trace, corresponding horizons, wavelet used and cross-correlation panel indicating the degree of the correlation coefficient.

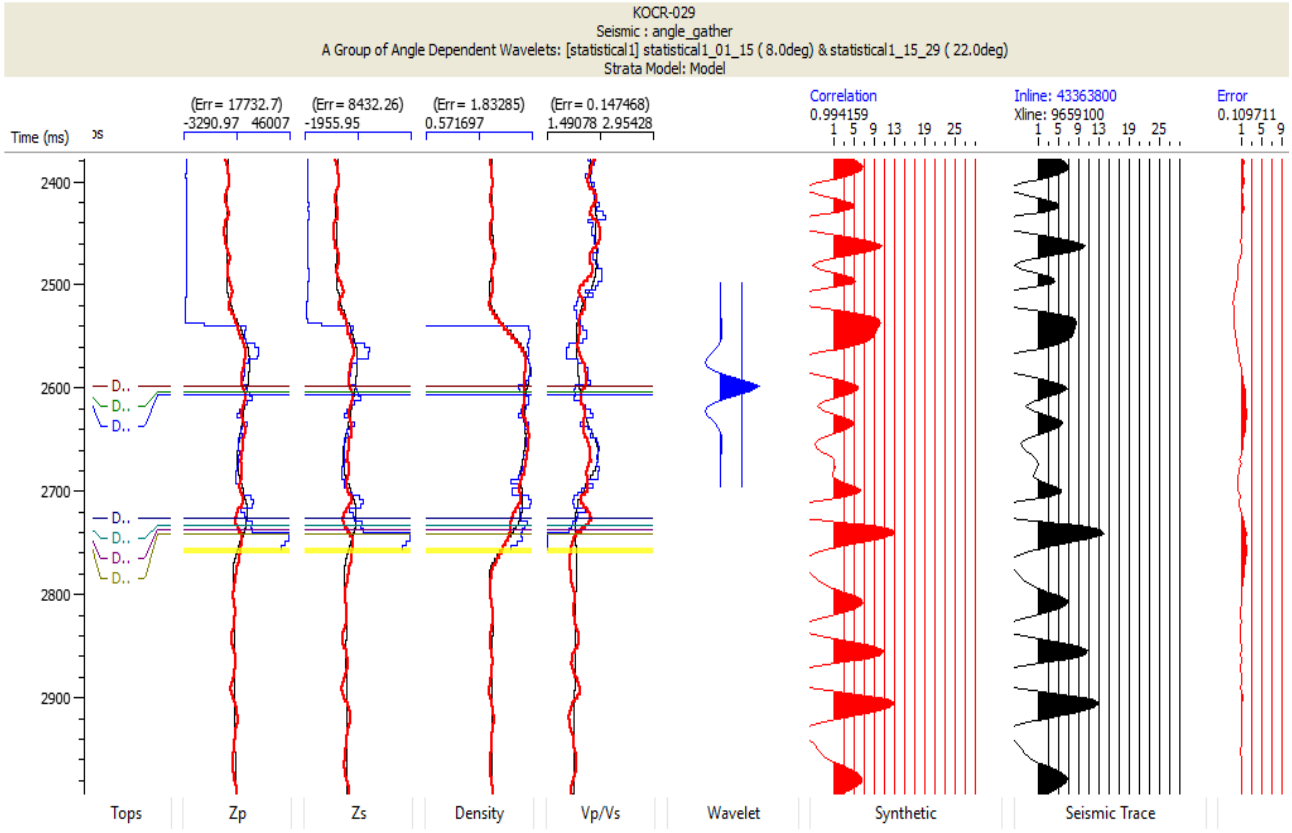

Figure 8. Inversion analysis for Well_001 showing reservoir tops, Zp (track 1), Zs (track 2), Density (track 3), Vp/Vs (track 4), synthetic trace (track 5), seismic trace (track 6) and error trace (track 7).

Results from the rock physics estimation from well data identified 2 reservoirs in Well 029 namely; HDZ1 and HDZ2 reservoirs which are made up of sub-reservoir D005, D006, D007 and D001, D002, D003, and D004 respectively. A horizon time slice of the HDZ2 horizon that cuts across the HDZ2 reservoir top was used for the inversion results.

4.2. Acoustic Impedance

The result from the inversion modelling shows that a low value of the acoustic impedance (Zp) reflects hydrocarbon-bearing reservoir while medium to high values represents brine and shale respectively. In the inverted section, the "HDZ2" reservoir is observed to be hydrocarbon-filled (Figure 9). However, a horizon time slice was generated from the HDZ2 horizon (Figure 10(a)), results from the slice divided the horizon into three zones namely; hydrocarbon-bearing zone, brine bearing zone and shale zone. These zones were identified by the values of acoustic impedance within the horizon with a hydrocarbon-bearing zone ranging from 19,743 to 20,487 (ft/s)(g/cc), and brine zone ranging from 20,487 to 22,531 (ft/s)(g/cc) and shale above 22531 (ft/s)(g/cc).

A 3D volume of acoustic impedance (Zp) was generated to identify hydrocarbon-filled sands across the field (Figure 10(b)). A time slice of 2875 ms was obtained. It was observed that the hydrocarbon-filled reservoir was mainly distributed

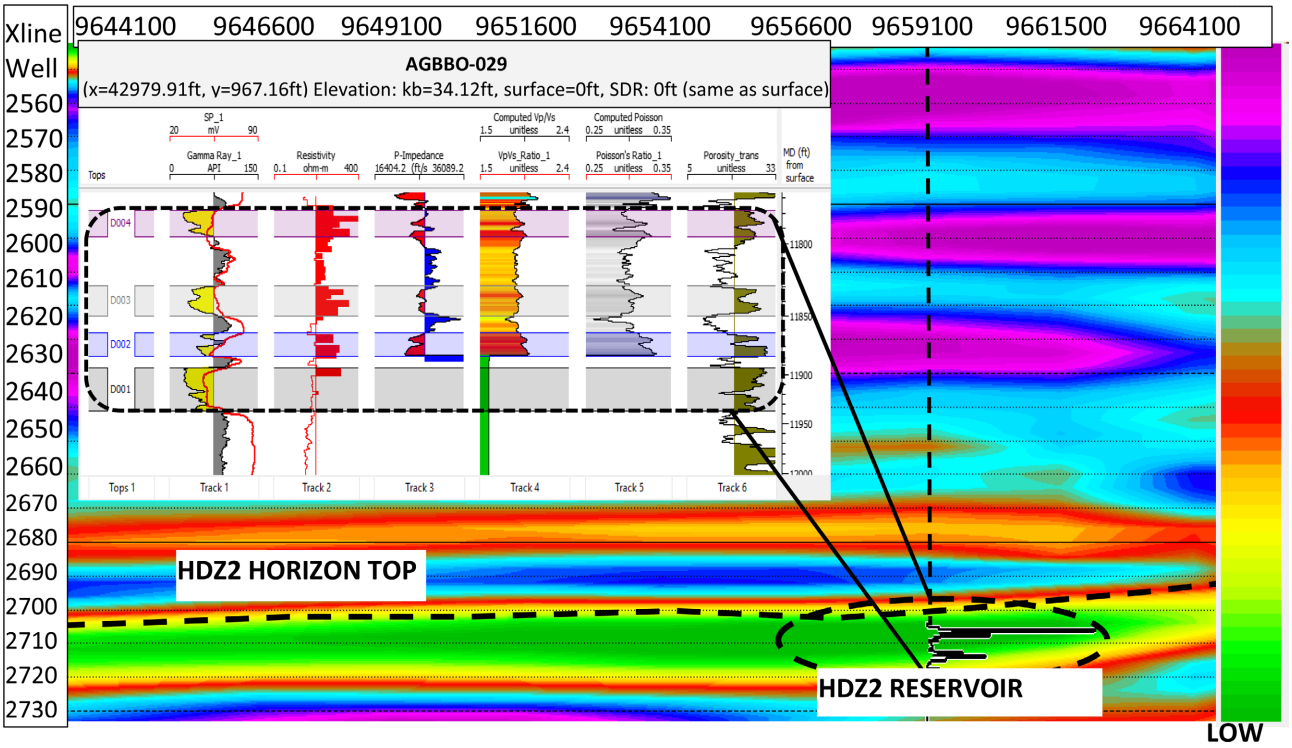

Figure 9. Crossline section showing inverted acoustic impedance with resistivity log inserted over the "HDZ2" reservoir around _029 and HDZ2 horizon top.

around the northeastern to southwestern trending meandering channel sands, which tend to be away from Well 029 well.

4.3. Primary and Shear Wave Velocity Ratio (Vp/Vs)

A result from the inversion modelling shows that the low value of velocity ratio (Vp/Vs) reflects sand interval while medium to high values represent shales. A horizon time slice was generated from the HDZ2 horizon (**Figure 11(a)**), results from the slice divided the horizon into two zones namely; the sand zone and the shale zone. These zones were identified by the values of Vp/Vs within the horizon with sand zone < 1.95 and shale zone > 1.95 (**Figure 11(a)**). However, a volume of Velocity ratio (Vp/Vs) was generated to identify sands and shale lithofacies across the field. A time slice of 2875 ms was obtained. The volume of VpVs ratio within the specified time slice shows that sand channels were mostly deposited on the northeastern part of the field as compared to the southern part dominated by shale intervals (**Figure 11(b)**).

4.4. Rigidity Modulus (Mu-Rho)

The result from the inverse modelling shows that a high value of rigidity modulus (Mu-Rho) reflects sand interval while medium to low values represent shales.

A horizon time slice was generated from HDZ2 as shown in **Figure 11**.

The results from the slice divided the horizon into two zones namely: the sand zone and the shale zone. These zones were identified by the values of Mu-Rho

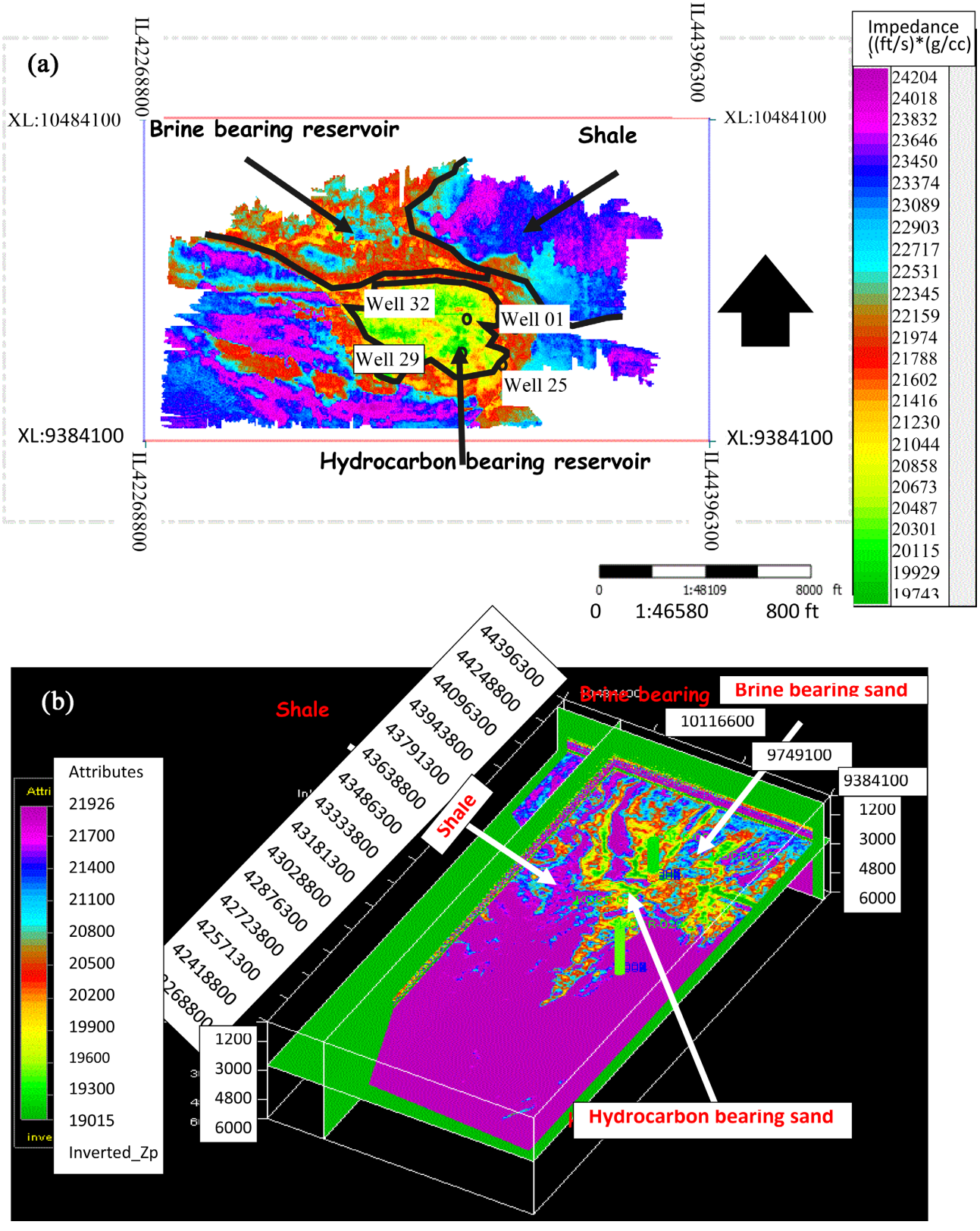

Figure 10. (a) Horizon slice of acoustic impedance across HDZ2 horizon showing hydrocarbon-filled sands, brine and shale and its corresponding well location. (b) 3D volume time slice of acoustic impedance at 2875 ms across the field showing hydrocarbon-filled sands at the North to Eastern part of the field.

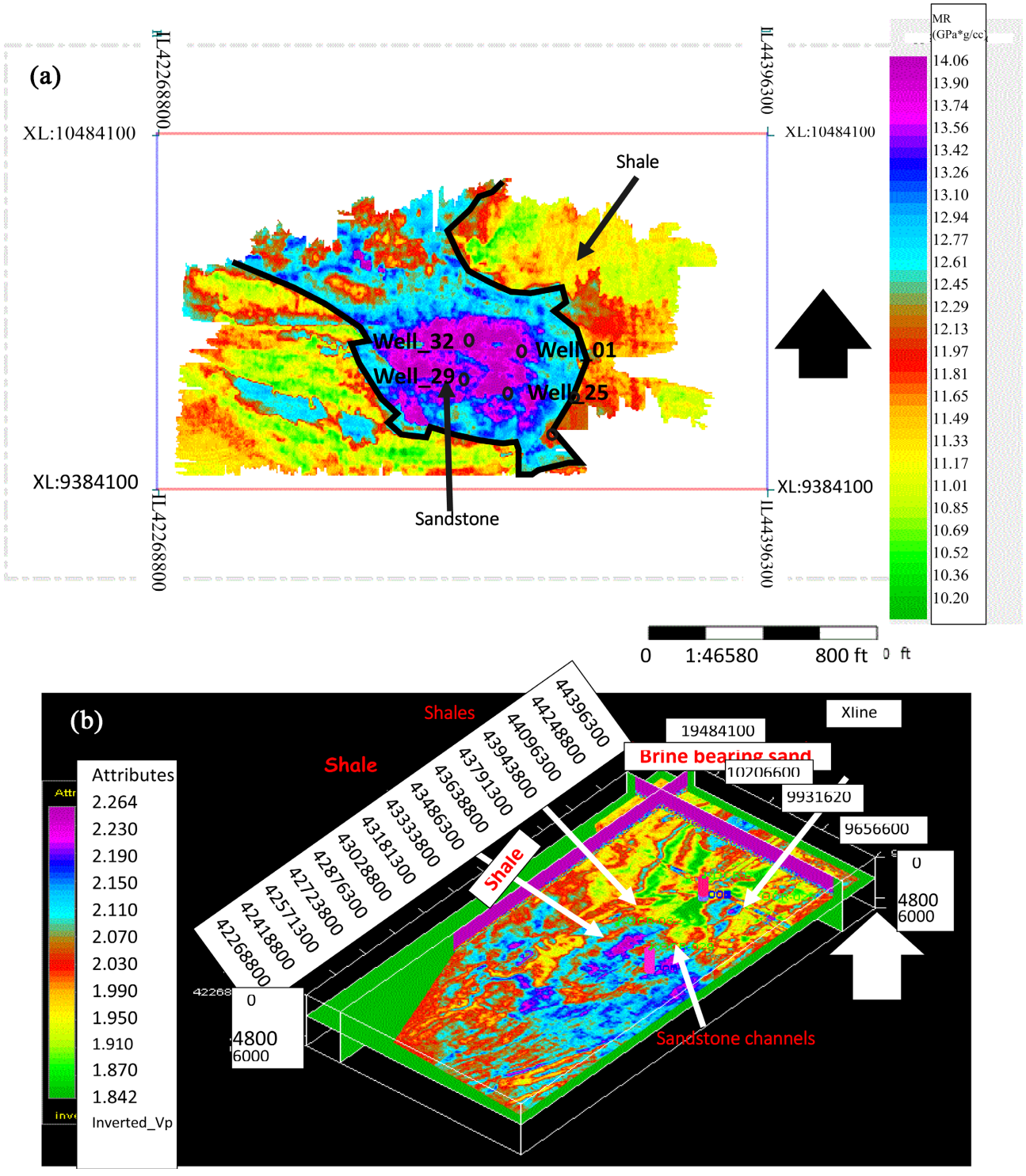

Figure 11. (a) Horizon slice of velocity ratio across HDZ2 horizon showing sands and shale and its corresponding well location. (b) 3D volume time slice velocity ratio at 2875 ms across the field showing hydrocarbon-filled sands at the North to Eastern part of the field.

within the horizon with sand zone ranging from 12.29 (GPa)(g/cc) and above and shale zone below 12.29 (GPa)(g/cc) (Figure 12(a)). However, a volume of rigidity modulus (Mu-Rho) was generated to identify sands and shale lithofacies

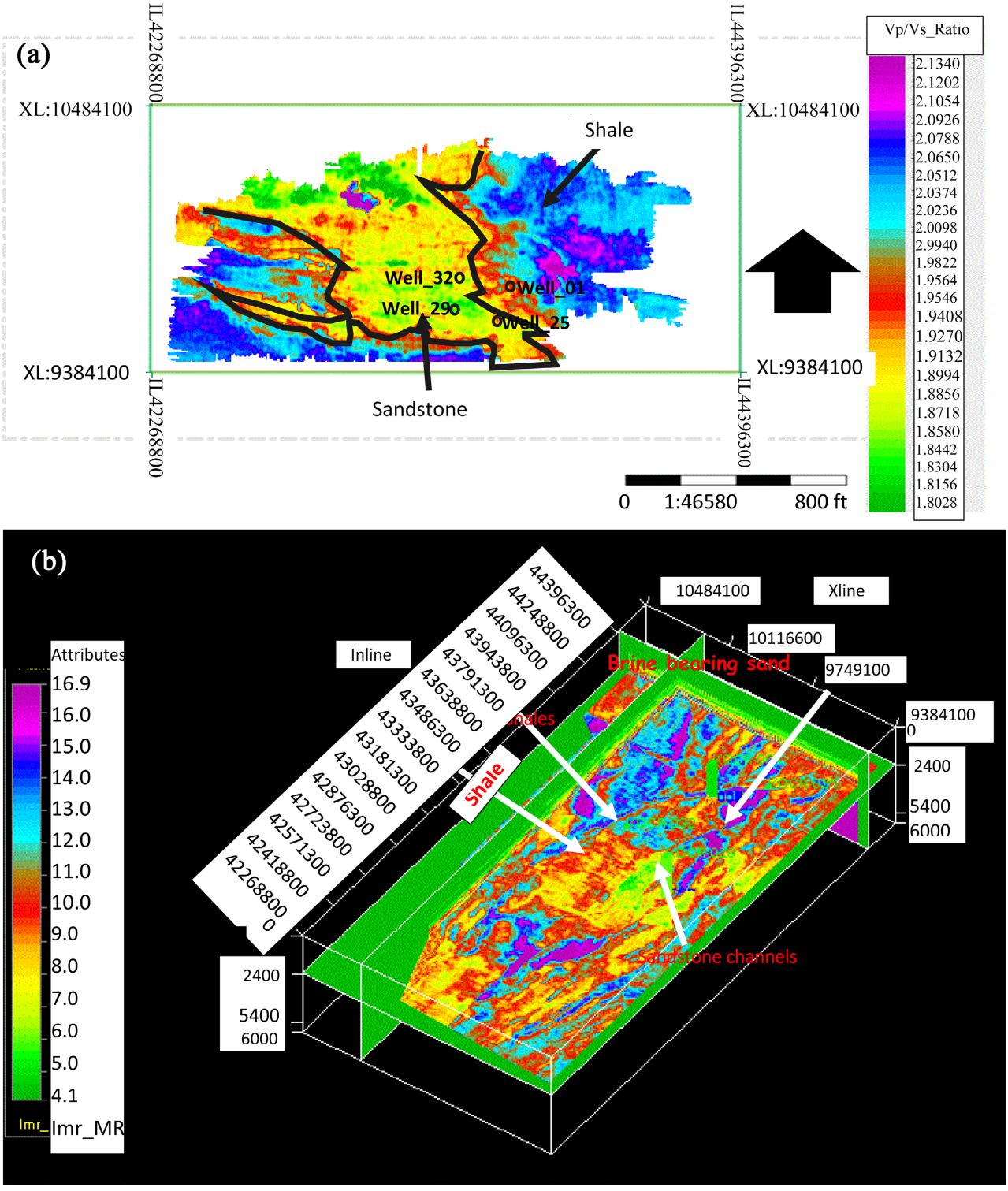

Figure 12. (a) Horizon slice of Mu-Rho across HDZ2 horizon showing sands and shale and its corresponding well location. (b) 3D volume time slice Mu-Rho at 2875 ms across the field showing hydrocarbon-filled sands at the North to East.

across the field. A time slice of 2875 ms was obtained. The volume of the Mu-Rho ratio within the specified time slice shows that sand channels were mostly deposited on the northeastern part of the field as compared to the south-

ern part dominated by shale intervals (**Figure 12(b)**).

5. Discussion

The study investigates an old marginal field, extending the applicability of simultaneous waveform inversion thus offers greater advantage than the conventional reservoirs study techniques. Tremendous achievements in the industry result from accurate litho-fluid predictions, which optimize exploration and production strategies.

We describe an inversion algorithm based on the Ma (2002) approximation, an improvement over the Aki-Richards approximation. Our goal is to find band-limited elastic reflectivities and integrate them into elastic properties. This involves merging reflectivities with their low-frequency counterparts and subjecting them to hard and soft constraints. Our approach builds upon earlier research that explored various inversion methods. By integrating rock physics principles with waveform inverse modeling, we enhance our understanding of reservoir properties.

Our results demonstrate the effectiveness of the modified Hashin-Shtrikman upper bound in distinguishing gas-filled reservoirs from brine-filled reservoirs and shale. Traditional petrophysical analysis struggles to achieve this level of discrimination. The approach is successfully applied across different well locations, serving as a model for predicting lithology and fluid types—a critical requirement for assessing geological variables (e.g., sorting, clay distributions) and optimizing production using time-lapse (4D) seismic interpretation.

Previous studies have highlighted the challenges of lithology and fluid-type characterization, especially in marginal fields. Traditional methods often lack precision, leading to uncertainties in reservoir assessment. Our work builds upon existing research by integrating rock physics principles with waveform inverse modeling. By doing so, we aim to enhance our understanding of reservoir properties and improve hydrocarbon exploration strategies. Our rock physics analysis identifies two primary reservoirs: HDZ1 and HDZ2. These reservoirs exhibit distinct acoustic impedance values, which serve as valuable indicators. Low acoustic impedance values are consistent with hydrocarbon-bearing reservoirs, while higher values correspond to brine and shale. The brine zone, specifically, falls within the range of 20,487 to 22,531 ft/s·g/cc, suggesting potential fluid-filled regions. In this study, lithofacies discrimination as one key objective of the study was achieved. Inversion analysis of Vp/Vs and Mu-Rho allows us to differentiate lithofacies. Sand and shale are the dominant lithologies. Sand is characterized by VpVs < 1.95, whereas shale exhibits VpVs > 1.95. Additionally, Mu-Rho values play a crucial role in lithofacies discrimination. Sands are associated with Mu-Rho > 12.29 GPa·g/cc, while shale values remain below this threshold.

Furthermore, the 3D volume analysis provides insights into the spatial distribution of hydrocarbons. A significant accumulation of hydrocarbons is observed

in the northern to eastern part of the field, forming a meandering channel. Sands are prevalent in the northeastern to southwestern regions, away from Well 029. This distribution pattern aligns with our lithofacies and fluid-type findings. In effect, by integrating rock physics and waveform inverse modeling, we enhance our ability to characterize reservoirs accurately. Our results contribute to improved reservoir management and guide exploration efforts in marginal fields.

The success of our approach also builds upon previous work by Ugbor and Onyeabor (2023), who evaluated spectral decomposition techniques in coastal swamp environments. Additionally, Ugbor et al. (2023) established prospectivity and risk assessment using seismic and petrophysical data in the Niger Delta. Our study complements these efforts by providing a robust method for lithofacies and fluid discrimination, bridging the gap between limited information and accurate reservoir characterization. By combining rock physics templates with Acoustic Impedance (AI) and porosity crossplots, we offer a practical solution for predicting lithology and fluid types in the Niger Delta basin. This approach contributes to reservoir management and facilitates informed decision-making for hydrocarbon exploration and production. The article thus builds upon earlier research that explored various inversion methods, including: Model-based inversion, Poisson impedance inversion, Deterministic and geostatistical inversion. However, the simultaneous waveform inversion method offers distinct advantages since it provides additional Information such as shear wave velocity data, enhancing reservoir discrimination, offers Wavelet effect Removal thereby improving image quality and provides a more comprehensive prediction since it predicts both lithology and fluids. Thus, our article refines inversion techniques and underscores the practical benefits of simultaneous waveform inversion for litho-fluid prediction. The work supports the estimating of Shear wave velocity after the work of Greenberg and Castagna, 1992.

6. Conclusion

The application of simultaneous waveform inversion was employed to predict lithology and fluid type across the "Agbbo" field, Niger Delta, Nigeria. Rock physics analysis identified 2 broad reservoirs, namely: HDZ1 and HDZ2 reservoirs. Results from the inversion modelling showed that the low value of the acoustic impedance (Zp) reflects hydrocarbon-bearing reservoir while medium to high values represent brine and shale respectively. From the inverted section, the "HDZ2" reservoir is observed to be hydrocarbon filled ranging from 19,743 to 20,487 (ft/s)(g/cc), brine zone ranging from 20,487 to 22,531 (ft/s)(g/cc) and shale above 22,531 (ft/s)(g/cc). Two lithofacies were identified from inversion analysis of Vp/Vs and Mu-Rho, namely: sand and shale with VpVs < 1.95 and >1.95 values respectively. Mu-Rho >12.29 (GPa)(g/cc) and <12.29 (GPa)(g/cc) represent sand and shale respectively. The 3D volume of acoustic impedance showed that the northern to the eastern part of the field is hydrocarbon bearing forming meandering channels. Velocity ratio and mu-rho identified the

northern to the eastern part of the field to be sandstone reservoirs and the southern to the western part of the field to be shales.

Acknowledgements

The authors acknowledge, with thanks, the efforts of the crew members of Felgra Links Nigeria Limited during the surface geophysical data acquisition and for providing the borehole logging data used for this study.

Conflicts of Interest

The authors declare no conflicts of interest regarding the publication of this paper.

References

Aki, K., & Richards, P. G. (1980). *Quantitative Seismology: Theory and Methods.* W. H. Freeman.

Akpan, A. S., Okeke, F. N., Obiora, D. N., & George, N. J. (2021). Modelling and Mapping Hydrocarbon Saturated Sand Reservoir Using Poisson's Impedance (PI) Inversion: A Case Study of Bonna Field, Niger Delta Swamp Depobelt, Nigeria. *Journal of Petroleum Exploration and Production, 11,* 117-132.

Chukwuemeka, P. A., Emele, U. O., & Ifenyinwa, O. A. (2018). Application of Rock Physics Parameters for Lithology and Fluid Prediction of "TN" field of Niger Delta Basin, Nigeria. *Egyptian Journal of Petroleum, 27,* 853-866. https://doi.org/10.1016/j.ejpe.2018.01.001

Doust, H., & Omatsola, E. (1989). Niger Delta: In J. D. Edwards, & P. A. Santogrossi (Eds.), *Divergent/Passive Margin Basins* (pp. 239-248). American Association of Petroleum Geologists Memoir. https://doi.org/10.1306/M48508C4

Ekwe, A. C., Onuoha, K. M., & Osanyande, N. (2012). *Fluid and Lithology Discrimination Using Rock Physics Modeling and Lambda-Mu-Rho Inversion: An Example from Onshore Niger Delta, Nigeria.* Search and Discovery Article #40865.

Eze M. O, Mode, A. W., Ugbor, C. C. (2013). Formation Evaluation of X7 Field in the Niger Delta: Evidence from Petrophysical Data. Niger Delta, Nigeria. *IOSR Journal of Applied Geology and Geophysics, 1,* 15-21. https://doi.org/10.9790/0990-0141521

Farfour, M., Yoon, W. J., & Kim, J. (2015). Seismic Attributes & Acoustic Impedance Inversion in Interpretation of Complex Hydrocarbon Reservoirs. *Journal of Applied Geophysics, 114,* 68-80. https://doi.org/10.1016/j.jappgeo.2015.01.008

Fatti, J. L., Smith, G. C., Vail, P. J., Strauss, P. J., & Levitt, P. R. (1994). Detection of Gas in Sandstone Reservoirs Using AVO Analysis: A 3-D Seismic Case History Using the Geostack Technique. *Geophysics, 59,* 1362-1376. https://doi.org/10.1190/1.1443695

Frankl, E. J., & Cordy, E. A. (1967). The Niger Delta Oil Province: Recent Developments Onshore and Offshore. In *Seventh World Petroleum Congress Proceedings* (pp. 195-209). WPC-12118. https://onepetro.org/WPCONGRESS/proceedings-abstract/WPC07/All-WPC07/WPC-12118/198886

Greenberg, M. L., & Castagna, J. P. (1992). Shear Wave Velocity Estimation in Porous Rocks: Theoretical Formulations: Preliminary Verification and Application. *Geophysical Prospecting, 40,* 195-209. https://doi.org/10.1111/j.1365-2478.1992.tb00371.x

Hampson, D. P., Russell, B. H., & Bankhead, B. (2005). Simultaneous Inversion of

Pre-Stack Seismic Data. In *75th SEG Meetings* (pp. 1633-1636). https://doi.org/10.1190/1.2148008

Horsfall, O., Omubo-Pepple, V., & Tamunobereton-Ari, I. (2014). Estimation of Shear Wave Velocity for Lithological Variation in the North-Western Part of the Niger Delta Basin of Nigeria. *American Journal of Scientific and Industrial Research, 5,* 13-22.

Lawrence, S. R., Munday, S., & Bray, R. (2002). Regional Geology and Geophysics of the Eastern Gulf of Guinea (Niger Delta to Rio Muni). *The Leading Edge, 21,* 1112-1117. https://doi.org/10.1190/1.1523752

llo, C. A., Ugbor, C. C., Eradiri, J. N., & Emedo, C. O. (2022). Prospect Identification and Reservoir Characterization Using Seismic and Petrophysical Data in "Famito" Field, Onshore Niger Delta. *Nigeria Arabian Journal of Geosciences, 15,* Article No. 348. https://doi.org/10.1007/s12517-022-09615-0

Ma, X. Q. (2002). Simultaneous Inversion of Pre-Stack Seismic Data for Rock Properties Using Simulated Annealing. *Geophysics, 67,* 1877-1885. https://doi.org/10.1190/1.1527087

Margrave, G. F., Lawton, D. C., & Stewart, R. R. (1998). Interpreting Channel Sands with 3C-3D Seismic Data. *The Leading Edge, 17,* 509-513. https://doi.org/10.1190/1.1438000

Moosavi, N., & Mokhtari, M. (2016). Application of Post-Stack and Prestack Seismic Inversion for Prediction of Hydrocarbon Reservoirs in a Persian Gulf Gas Field. *International Journal of Environment, Chemistry, Ecology, Geophysics and Engineering, 10,* 853-862.

Nwogbo, P. O., Omudu, M., Dike, R., Olotu, S., & Osayande, N. (2009). Seismic-Based Lithology and Fluid Delineation of the ROK Reservoir Sand, Shallow Offshore Niger Delta. In *SEG Technical Program Expanded Abstracts 2009* (pp. 608-612). https://doi.org/10.1190/1.3255830

Okeugo, C. G., Onuoha, K. M., Ekwe, C. A., Anyiam, O. A., & Dim, C. I. P. (2018). Application of Crossplot and Prestack Seismic-Based Impedance Inversion for Discrimination of Lithofacies and Fluid Prediction in an Old Producing Field, Eastern Niger Delta Basin. *Journal of Petroleum Exploration and Production Technology, 9,* 97-110. https://doi.org/10.1007/s13202-018-0508-6

Omudu, L. M., Ebeniro, J. O., Xynogalas, M., Adesanya, O., & Osayande, N. (2007). Beyond Acoustic Impedance: An Onshore Niger Delta Experience. In *SEG/San Antonio Annual Meeting* (pp. 412-415). https://doi.org/10.1190/1.2792453

Othman, A. A., Ewida, F., Fathi, M. A., & Embaby, M. A. (2015). Seismic Inversion for Reservoir Characterization in Komombo Basin, Upper Egypt, (Case Study). *International Journal of Innovative Science, Engineering & Technology, 2,* 654-666.

Reijers, T. J. A. (2011). Stratigraphy and Sedimentology of the Niger Delta. *Geologos, 17,* 133-162. https://doi.org/10.2478/v10118-011-0008-3

Reijers, T. J. A., Petters, S. W., & Nwajide, C. S. (1996). The Niger Delta Basin. *Sedimentary Basins of the World, 3,* 151-172. https://doi.org/10.1016/S1874-5997(97)80010-X

Short, K. C., & Stauble, A. J. (1967). Outline of the Geology of Niger Delta. *American Association of Petroleum Geologists Bulletin, 51,* 761-779. https://doi.org/10.1306/5D25C0CF-16C1-11D7-8645000102C1865D

Tian L., Zhou D., Lin G., & Jiang L. (2010). Reservoir Prediction Using Poisson Impedance in Quinhuangdao, Bohai Sea, In *SEG Denver 2010 Annual Meeting* (pp. 2261-2264). https://doi.org/10.1190/1.3513300

Ugbor, C. C. (2023). Evaluation of Hydrocarbon Reservoir in the "SIMA" Field of Niger Delta Nigeria from Interpretation of 3D Seismic and Petrophysical Log Data. *Interna-*

tional Journal of Geosciences, 14, 94-107. https://doi.org/10.4236/ijg.2023.141006

Ugbor, C. C., & Onyeabor, S. O. (2023). Assessment of the Spectral Decomposition Techniques in the Evaluation of Hydrocarbon Potential of "BOMS" Field, Coastal Swamp Niger Delta, Nigeria. *International Journal of Geosciences, 14,* 655-676. https://doi.org/10.4236/ijg.2023.147035

Ugbor, C. C., Ugwuoke, C. I., & Odong, P. O. (2023). Hydrocarbon Prospectivity and Risk Assessment of "Bob" Field Central Swamp Depobelt, Onshore Niger Delta Basin, Nigeria. *Open Journal of Geology, 13,* 847-882. https://doi.org/10.4236/ojg.2023.138038

Veeken, P. C., & Da Silva, M. (2004). Seismic Inversion Methods and Some of Their Constraints. *First Break, 22,* 47-70. https://doi.org/10.3997/1365-2397.2004011